lncRNA *NORM* is essential for proper chromosome segregation through the Plk1-Bub1 and Nsun2 axis.

Vikas Dongardive[1,2], Sonali Jathar[1], Juhi Srivastava[1] and Vidisha Tripathi[1*]

[1]Laboratory of lncRNA Biology, National Centre for Cell Science, NCCS Complex, Pune University Road, Pune-411007, MH, INDIA

[2]Department of Biochemistry and Molecular Biology, College of Medicine, University of Florida, Gainesville, FL, USA.

*Address correspondence to: Vidisha Tripathi (tvidisha@nccs.res.in)

Abstract:

The cell cycle comprises different phases and is a tightly regulated process at the molecular level. During the cell cycle, two key events occurred: DNA duplication during the S phase and chromosome segregation during mitosis. Accurate cell cycle progression, achieved through faithful chromosome segregation, is essential for maintaining cell fidelity. Long noncoding RNAs are a subclass of noncoding RNA that are longer than 200 bp and form RNA protein complexes (RNPs) to regulate various biological processes. Herein, we demonstrate that lncRNA *NORM* is involved in regulating the cell cycle by maintaining proper chromosome segregation. *NORM* exhibited G2 phase-specific expression, and the depletion of *NORM* resulted in a significant G2/M arrest. *NORM*-depleted cells failed to progress in mitosis and showed defects in chromosome segregation. We further demonstrated that *NORM* binds to proteins such as Plk1 and Nsun2. Depletion of *NORM* hindered the interaction between Plk1 and Bub1, resulting in reduced kinetochore localization of Plk1 during prometaphase. Our results also show that the depletion of *NORM* affects the binding of Nsun2 protein to CDK1 mRNA and, consequently, the stabilization of CDK1 at the protein level. Altogether, our results demonstrate that *NORM* regulates chromosome segregation by mediating the interaction between Plk1 and Bub1.

Keywords: long noncoding RNA, cell cycle, chromosome segregation, Plk1, Bub1, Mitosis.

60 **Introduction:**

61 The mammalian cell cycle is a ubiquitous and tightly regulated process that comprises events
62 orchestrated in an orderly manner to culminate in the formation of two daughter cells. Entry of
63 a cell into different phases of the cell cycle is precisely controlled by the complex of oscillating
64 concentrations of different Cyclins and CDK complexes. In addition to Cyclins and CDKs,
65 various cyclin kinase inhibitors (CKIs) and cell cycle regulatory proteins, such as RB, p53, and
66 p21, are also involved in regulating the cell cycle (1,2). Two key events that occur during the
67 cell cycle are the duplication of genetic material in the S phase and the segregation of
68 chromosomes in the M phase. Precise control of chromosome segregation during the M phase
69 is crucial for error-free cell cycle progression, as any defect in chromosome segregation can
70 lead to cellular abnormalities that ultimately contribute to the development of various cellular
71 disorders, including cancer (3). One of the key events that is responsible for faithful
72 chromosome segregation is the attachment of the kinetochore to microtubules (KT-MT) (4). A
73 plethora of proteins are involved in mediating the proper attachment of KT-MT for the
74 segregation of chromosomes. Any defect in chromosome segregation is detected by the
75 surveillance mechanism known as the spindle assembly checkpoint (SAC), which is activated
76 to correct the erroneous microtubule-to-kinetochore attachment (5). Budding uninhibited by
77 benzimidazoles 1 (Bub1) plays a pivotal role in assembling the SAC complex by localizing at
78 the kinetochore through the phosphorylation of Knl1 by Mps (6,7). Phosphorylated Knl1 then
79 recruits the Bub3-Bub1 complex. Additionally, Mps1 phosphorylates Bub1 to mediate its
80 interaction with the Mad1-Mad2 complex, thereby creating a SAC signaling platform (8). This
81 platform then further recruits Bub3, BubR1, Cdc20, and Mad2. Bub1 also binds to another
82 kinase, Polo-like kinase 1 (Plk1), and the interaction between Plk1 and Bub1 is essential for
83 the kinetochore localization of Plk1. Any defects in Plk1 kinetochore localization cause
84 chromosome mis-segregation, marked by chromosomes associated with spindle poles (9).
85 The interaction between Bub1 and Plk1 primarily depends on Bub1's phosphorylation at T609,
86 mediated by the CDK1 protein (9). The Cyclin B and CDK1 complex drives the entry of a cell
87 into mitosis and is crucial for guaranteeing accurate and faithful segregation of duplicated
88 chromosomes. CDK1 is also regulated by various proteins, such as MYT1 and WEE1, which
89 deactivate CDK1 through phosphorylation (10,11). Moreover, CDK1 is also regulated through
90 mRNA stabilization by the protein binding to its mRNA. NOP2/Sun RNA methyltransferase
91 family, member 2 (NSun2) (Misu) stabilizes CDK1 and enhances its translation by binding to
92 its mRNA and methylating its 3' untranslated region (UTR) (12). CDK1 binds to Cyclin B and
93 becomes activated. Upon activation, it phosphorylates a variety of substrates, including Bub1,
94 which is crucial for mitosis and contributes to the faithful segregation of chromosomes. Multiple
95 lines of evidence suggest that noncoding RNAs, including microRNAs (miRNAs) and long

96 noncoding RNAs (lncRNAs), are also involved in regulating the cell cycle. lncRNAs are a class
97 of noncoding RNAs that are longer than 200 bp and characterized by their short open reading
98 frame. By forming RNP complexes, lncRNAs are known to control a variety of biological
99 processes through Signal, decoy, Guide, or Scaffold mechanisms. In a recent study, it has
100 been demonstrated that lncRNA MALAT1 is differentially regulated during the G1/S and M
101 phases and is essential for the progression of the cell cycle from G1/S to S and from G2 to M,
102 through the transcription and alternative splicing of the gene bMyb (13). Another study has
103 demonstrated that the lncRNA EMS controls the cell cycle progression during the G1/S phase.
104 EMS stabilizes E2F1 mRNA by binding to the RALLY protein in a manner that increases the
105 expression of that gene (14). lncRNAs also interact with CDKs to regulate cell cycle
106 progression. A recent study revealed that lncRNA HOXC-AS3 interacts with CDK2, thereby
107 facilitating reduced binding of CDK2 to p21, which ultimately leads to increased CDK2 activity
108 and promotes cell proliferation (15). Several other studies have demonstrated that many long
109 noncoding RNAs (lncRNAs) play a role in cell cycle regulation. However, a thorough
110 investigation of novel lncRNAs involved in controlling the cell cycle program is lacking.
111 Understanding the involvement of lncRNAs in cell cycle regulation will provide a detailed
112 molecular mechanism and open up new opportunities for novel treatments of cellular disorders
113 associated with cell cycle dysregulation.

114 In this study, we showed the involvement of *NORM* in regulating the cell cycle. We
115 demonstrated that a novel long noncoding RNA, *NORM* (Noncoding RNA Regulator of
116 Mitosis), is crucial for proper chromosomal segregation by modulating the interaction between
117 Plk1 and Bub1. *NORM* is a G2-phase enriched lncRNA and is essential for driving the G2/M
118 progression of the cell. *NORM* depletion causes G2/M arrest of cells marked with chromosome
119 misalignment, which ultimately results in cell apoptosis. The interaction between Plk1 and
120 Bub1 is hampered upon *NORM* depletion. We have demonstrated the molecular relationship
121 between *NORM* and another protein, Nsun2. Additionally, we have demonstrated that *NORM*
122 depletion reduces the binding of Nsun2 to CDK1 mRNA, thereby decreasing the stability of
123 the CDK1 protein. We observed that a reduced level of CDK1 protein results in a decrease in
124 the phosphorylation of Bub1 at T609. Finally, Plk1 localization at the kinetochore is altered as
125 a result of hindering the interaction between Plk1 and Bub1. Overall, our research suggests
126 that the novel lncRNA *NORM* plays a crucial role in regulating the cell cycle by ensuring normal
127 chromosome segregation.

128

129 **Results:**

130 ***NORM* is upregulated during the G2 phase of the cell cycle and promotes G2/M**
131 **transition**

132 The cell cycle is a more complex phenomenon that is coordinated through multiple layers of
133 regulation, driven by proteins as well as a wide array of noncoding RNAs, including long
134 noncoding RNAs (lncRNAs) and microRNAs (miRNAs). One of our comprehensive studies
135 has identified a set of cell cycle-related long noncoding RNAs (lncRNAs), with most of these
136 lncRNAs exhibiting cell cycle phase-specific expression patterns. lnc00667 is one such
137 lncRNA that showed G2 phase-specific expression in synchronized HeLa cells. Based on its
138 function, we named lnc00667 the Noncoding RNA Regulator of Mitosis *(NORM). NORM* is
139 approx. 4.0 nucleotides long noncoding transcript located on chromosome 18
140 (chr18:5,232,875-5,290,608 (GRCh38/hg38)), Histone tail modification map indicated a
141 significant H3K4me3 and H3K27ac marks on the promoter of *NORM*, indicating that it is
142 actively transcribed across different cell types **[FIG 1A].** The coding probability of the *NORM*
143 transcript was analyzed using the CPAT tool, revealing that *NORM* does not code for any
144 protein, unlike the well-characterized long noncoding RNA MALAT1 **[FIG. 1B].** To understand
145 its cis-acting or trans-acting mode, *NORM* was further characterized for its subcellular
146 localization using a subcellular fractionation method, followed by a quantitative real-time PCR
147 analysis to assess the level of *NORM*. Quantitative real-time PCR data revealed that *NORM*
148 is predominantly located in the nucleus, with some fraction also present in the cytoplasm **[FIG.**
149 **1C].** Quantitative real-time PCR (qRT-PCR) analysis revealed that the transcript levels of
150 *NORM* remain low during the G1 and S phases of the cell cycle. However, there is a steady
151 increase in transcript levels during the G2 phase, followed by a subsequent decrease in the
152 M phase **[FIG. 1D].** Cell cycle phase-specific expression of lncRNAs is often associated with
153 their role in that specific phase. An elevated level of *NORM* in the G2 phase suggests its
154 potential role in regulating G2/M progression. To understand whether *NORM* is required for
155 normal cell cycle progression and to examine the functional relevance of *NORM*, Antisense
156 oligonucleotide (ASO)- based depletion of *NORM* was performed followed by cell cycle
157 analysis by using propidium iodide (PI) based fluorescence activated cell sorting (FACS) which
158 showed a significant G2/M arrest in asynchronously growing WI-38 cells **[FIG. 1E, F, and H]**.
159 The effect of *NORM* depletion on cell cycle progression was further confirmed by performing
160 BrdU-PI flow cytometry. We observed a significant increase in the G2/M population upon
161 *NORM* depletion, confirming that *NORM* depletion leads to cell cycle arrest at the G2/M phase
162 **[FIG. G]**. It was evident from the cell cycle analysis that the absence of *NORM* caused a
163 significant G2/M arrest in the cell cycle, indicating the importance of *NORM* in driving cells
164 through the G2/M phase. We further confirmed the role of *NORM* in driving G2/M progression
165 by arresting the asynchronously growing HeLa cells in mitosis with Nocodazole treatment,

166 followed by subsequent release in control and *NORM*-depleted conditions, and then analyzed
167 by PI-FACS. PI-flow cytometry analysis indicated that in the control condition, cells were
168 correctly arrested upon nocodazole treatment and subsequently progressed from the G2/M
169 phase to the G1 phase upon release. Nevertheless, in the *NORM* depletion condition, cells
170 failed to progress from the G2/M phase to the G1 phase even after 10 hours of release **[FIG.**
171 **1I & J].** Moreover, we observed that the level of CDK1 was reduced upon *NORM* depletion
172 compared to the control, as determined by our immunoblot analysis **[Fig. 1K]**. This indicates
173 the importance of *NORM* in driving the cells through the G2/M phase. As DNA content-based
174 cell cycle analysis is incapable of distinguishing between the G2 and M-phase populations,
175 we employed H3ser10 phosphorylation-based cell cycle analysis. A close examination of G2
176 and M phase populations revealed that *NORM* depletion results in a substantial decrease in
177 the mitotic phase population and an increase in the G2 phase population, indicating a failure
178 of the cells to progress from the G2 to the M phase **[FIG. 1 L&M]**. This was further confirmed
179 by immunoblotting analysis, which checked the level of phospho-H3 at the ser10 residue. The
180 level of phospho-H3 (ser10) was significantly reduced upon *NORM* depletion **[FIG. 1 N]**.

181 **Loss of *NORM* affects cellular proliferation, leading to an increase in apoptosis.**

182 Depletion of *NORM* resulted in a marked increase in the G2/M population, prompting us to
183 investigate the effect of *NORM* on cellular proliferation. The effect on proliferation was
184 evaluated by performing Ki-67 immunostaining. The results showed a considerable decrease
185 in Ki-67-positive cell numbers in *NORM*-depleted conditions compared to control conditions
186 **[FIG. 2A & B]**. *NORM* depletion resulted in a substantial reduction in cellular viability and
187 proliferation, as well as a significant decrease in colony formation ability, as observed through
188 the MTT assay and clonogenic assay, respectively, confirming the observations about
189 proliferation **[FIG 2C, D, and E].** This data revealed that *NORM* depletion significantly reduced
190 cell proliferation, suggesting that *NORM* depletion can lead to defects in cell cycle progression.
191 The cell cycle analysis data showed an increase in the sub-G1 population upon *NORM*
192 depletion, indicating a significant level of apoptosis in the absence of the lncRNA. We then
193 determined the level of apoptosis in *NORM*-depleted cells by performing Annexin V-FITC and
194 propidium iodide (PI) based flow cytometry. The flow cytometry data showed an increase in
195 early and late apoptotic populations upon *NORM* depletion compared to those in control cells
196 **[FIG. 2E & F].** Increased levels of cleaved PARP in *NORM*-depleted conditions further
197 validated the result. Additionally, anti-apoptotic protein Bcl2 levels were decreased, while pro-
198 apoptotic protein Bax levels were increased upon *NORM* depletion **[FIG. 2G].** The overall data
199 suggests the importance of *NORM* in promoting cellular proliferation and inhibiting apoptosis.

Loss of *NORM* results in changes in gene expression at the global transcriptomic and proteomic levels.

To understand the molecular mechanism underlying the cell cycle defect upon *NORM* depletion, we analyzed gene expression changes by performing a global transcriptome analysis on control and *NORM*-depleted samples using the Illumina HiSeq 2500 platform. Global transcriptome profiling revealed that the loss of *NORM* results in the differential expression of 1,050 genes, wherein nearly 500 genes showed more than 2.5-fold up-regulation, while 550 genes showed more than 2.5-fold down-regulation **[FIG. 3A]**. ZNF48, SLC16A6, BRCA1, CHRND, PCNT, DCAKD, POT1, ZNF74, RNF14, and YY1AP1 were the top down-regulated genes, while SEC31A, ITGA2, FBXO6, DNM2, SMURF1, GUCD1, WDR4, POP1, PPP1R7, and PSMD1 were the top up-regulated genes **[Supplementary 3.1]**. Using qRT-PCR, we validated the expression of several differentially expressed genes (DEGs), which showed a similar trend **(Supplementary 3.2).** We next analysed the effect of *NORM* on cellular biological pathways by performing gene ontology analysis. Gene ontology revealed that many cell cycle-related biological processes and pathways were affected by *NORM* depletion. The top ten down-regulated biological processes and upregulated biological processes include cell cycle-related pathways such as regulation of mitotic cell cycle phase transition, regulation of cell cycle phase transition, positive regulation of cell cycle, G2/M transition of the mitotic cell cycle, cell cycle G2/M phase transition **[FIG 3B &C]**. The down-regulation of G2/M transition-related genes, such as MELK, CEP70, CDK2, PPP2R2A, PCNT, and CDC25A, suggests a failure in the G2/M transition in the absence of *NORM*. To gain further insight, we performed a proteomics analysis in *NORM*-depleted and control conditions to check the effect of *NORM* depletion on different proteins and biological processes. *NORM* depletion resulted in > 2-fold down-regulation of 146 proteins and > 2-fold up-regulation of 679 proteins **[FIG 3D].** Many cell cycle-related proteins showed differential expression. Proteins known for their role in cell cycle regulation, such as TGM2, PSMD, CLTC, PSMD2, BUB3, and ANXA4, were significantly upregulated. In contrast, proteins such as PDGFRB, PTMS, COL1A1, CD2AP, LAMB2, YWHAB, CDK1, MCM3, and YWHAG were significantly reduced upon *NORM* depletion **[Fig. 3E].** To further understand this, we performed a Gene Ontology (GO) analysis of proteomics data using the DAVID tool. The gene ontology analysis of the proteomics data revealed that biological processes, such as “negative regulation of ubiquitin-protein ligase activity involved in mitotic cell cycle, anaphase-promoting complex-dependent catabolic process, mitotic nuclear envelope disassembly, mitotic spindle assembly, Cell cycle, and G2/M transition of the mitotic cell cycle,” were affected **[Fig. 3F].** The Gene Ontology data suggest that *NORM* is involved in regulating mitosis-related pathways. Global transcriptome and proteomics profiling data indicate an overlap between RNA-seq and proteomics profiles.

236 Altogether, our high-throughput data suggest the importance of *NORM* in regulating the cell
237 cycle by associating with mitosis-related pathways.

238 ***NORM* interacts with cell cycle regulatory proteins for chromosome segregation and**
239 **cell cycle regulation**

240 We next sought to investigate the mechanism of action of *NORM* in regulating the cell cycle.
241 We incubated the *in vitro* transcribed full-length biotinylated *NORM* with cell lysate, followed
242 by a pulldown of the *NORM*-protein complex using streptavidin beads **[FIG. 4A]**. *NORM*
243 showed interaction with numerous proteins, including cell cycle regulatory proteins CALM2,
244 CDC5L SPOUT1, KHDRBS1, Nsun2 and Plk1, out of which polo-like kinase 1 (Plk1) seemed
245 to be interesting as Plk1 is required for entry of cells into mitosis and our previous results
246 observed a defect in G2/M transition in *NORM* depletion conditions **[FIG 4B &C]**. The *NORM*-
247 Plk1 interaction was confirmed by performing RNA immunoprecipitation, which showed
248 significant enrichment (~3-fold) of *NORM* in the Plk1 immunoprecipitated **[FIG. 4D]**.
249 Interestingly, we also observed a marginal decline in Plk1 protein levels upon *NORM* depletion
250 **[FIG. 4E]**. Plk1 is one of the major kinases in mitosis, phosphorylating a multitude of substrates
251 at various subcellular locations to regulate mitotic events. Plk1 is essential for the proper
252 assembly of spindles, centrosome maturation, and the attachment of microtubules to
253 kinetochores. We then investigate the role of *NORM* on Plk1's localization at different
254 subcellular locations. We observed differential localization of Plk1 at various subcellular
255 locations, with some defects, in the *NORM*-depleted condition **[FIG. 4F].** To understand the
256 role of *NORM* on Plk1 localization at kinetochores and centrosomes, we examined the level
257 of Plk1 at kinetochores in control versus *NORM* depletion conditions using
258 immunofluorescence. We observed a significantly reduced intensity of Plk1 at kinetochores
259 upon *NORM* depletion compared to control cells, suggesting that *NORM* depletion affected
260 Plk1 localization at kinetochores **[FIG. 4 G&H].** We next sought to determine the effect of
261 *NORM* depletion on chromosome segregation. We observed that depletion of *NORM* leads to
262 defective chromosome segregation, marked by the misalignment of chromosomes during
263 mitosis, and a significantly higher number of cells showed lagging chromosomes at the spindle
264 pole **[Fig. 4 I & J]**.
265

266 ***NORM* depletion hampered the interaction between PLK1 and Bub1**
267 Next, to elucidate the mechanism of reduced localization of Plk1 at kinetochores, we examined
268 the effect of *NORM* depletion on the interaction of key regulatory proteins involved in mitosis.
269 With the help of string analysis, we found that many cell cycle regulatory proteins, such as
270 cyclin B, CENP-E, and Bub1, are known to interact with Plk1 **[FIG. 5A]**. The interaction
271 between Bub1 and Plk1 is crucial for the localization of Plk1 at kinetochores. Plk1 interacts

with Bub1 through its polo-box domain (PBD) and phosphorylates Bub1**.** First, we checked if there was any effect of *NORM* depletion on the level of Bub1. We checked the kinetochore localization of Bub1 in control and *NORM*-depleted cells. We observed a marginal change in Bub1 intensity at the kinetochore upon *NORM* depletion **[FIG. 5B & C]**, and no significant change was observed at the protein level of Bub1 upon *NORM* depletion **[FIG. 5D]**. We then checked the effect of *NORM* on the interaction between Plk1 and Bub1. Interestingly, when we immunoprecipitated Plk1, it was able to co-immunoprecipitate Bub1 along with it; however, upon *NORM* depletion, the interaction between Plk1 and Bub1 was hampered, as Plk1 failed to co-immunoprecipitate Bub1 **[FIG. 5E]**. The interaction was validated by performing reverse Co-immunoprecipitation in which an antibody against Bub1 was used to immunoprecipitate Bub1. Reverse Co-IP also showed that upon *NORM* depletion, the interaction between Plk1 and Bub1 was hampered **[FIG. 5F]**. It is known that CDK1 phosphorylates Bub1 at the T609 residue, and this phosphorylation is essential for the interaction between PLK1 and Bub1 (16)**.** A mitosis-specific anti-MPM2 antibody can be used to detect Bub1 phosphorylated at the T609 residue, and phosphorylation of Bub1 at T609 is crucial for the Plk1-Bub1 interaction and the localization of Plk1 at the kinetochore (17)**.** Considering the importance of Bub1 T609 in Plk1 interaction, we checked the effect of *NORM* depletion on Bub1 phosphorylation. We immunoprecipitated Bub1 using an anti-Bub1 antibody and assessed the phosphorylation status of Bub1 at T609 using an anti-MPM2 antibody. Interestingly, we observed that *NORM* depletion led to a significant reduction in Bub1 phosphorylation at the T609 residue **[FIG. 5G & H]**, indicating that *NORM* is involved in mediating Bub1 phosphorylation. The depletion of *NORM* led to a decrease in Bub1 phosphorylation, which ultimately hindered Bub1's interaction with Plk1**.** Altogether, these results suggest that the *NORM* is involved in mediating the interaction between Plk1 and Bub1 through the phosphorylation of Bub1 at T609.

***NORM* mediates the binding of Nsun2 on CDK1 mRNA to stabilize CDK1 protein**

We investigated Bub1's upstream targets to gain a deeper mechanistic understanding of how *NORM* regulates the phosphorylation of Bub1. It is known that Bub1 is phosphorylated at T609 by cyclin-dependent kinase 1 (CDK1). Therefore, we explore any potential association between *NORM* and CDK1. Our RNA pulldown data showed that *NORM* lncRNA also interacts with the tRNA methyltransferase Nsun2 (Misu). We validated this interaction by performing an RNA pulldown followed by western blotting to verify the presence of Nsun2 **[Fig. 6A]**. Nsun2 binds to CDK1 mRNAs. It stabilizes them at the protein level by methylating them. Next, we examined the effect of *NORM* depletion on Nsun2 at the protein level**.** We found no apparent change in Nsun2 at the protein level, indicating that *NORM* does not directly control Nsun2

expression **[Fig. 6B].** Next, we examined the effect of *NORM* depletion on Nsun2 binding to CDK1 mRNA with RNA-immunoprecipitation **[Fig. 6D]**. Interestingly, our RNA-IP with anti-Nsun2 antibody showed that upon depletion of NORM, CDK1 enrichment on Nsun2 was considerably lower than in control cells **[Fig. 6D].** These results suggested that *NORM* depletion inhibits Nsun2's propensity to bind to CDK1 mRNA. Next, we checked the effect of reduced binding on CDK1 protein level immunoblotting data suggested that the CDK1 was reduced at the protein level upon *NORM* depletion **[Fig 6E],** suggesting that the reduced level of Nsun2 binding of CDK1 mRNA hampered by *NORM* depletion, and hence it resulted in reduced stability of CDK1 protein. This reduced level of CDK1 resulted in decreased phosphorylation of Bub1 at T609, ultimately hindering the interaction between Plk1 and Bub1. Overall, the evidence suggests the necessity of *NORM* for chromosomal segregation and normal cell cycle progression by mediating Nsun2's binding to CDK1 mRNA and modulating the interaction between Bub1 and Plk1.

Discussion:

In this study, we have demonstrated that *NORM*, a long noncoding RNA, plays a crucial role in regulating cell cycle progression from the G2 to M phase. We observed that *NORM* shows an elevated level of expression in the G2 phase. Multiple studies have demonstrated that lncRNAs exhibit tissue- and cell-stage-specific expression. This tissue- and cell-specific expression is often associated with the function of lncRNAs in that cell or tissue. The Kannanganattu V Prasanth group has demonstrated that more than 2,000 long noncoding RNAs (lncRNAs) exhibit periodic expression during the cell cycle. (18). An elevated level of lncRNA is found to be associated with cell stage-specific regulation of the cell cycle phases in a cell stage-specific manner. Therefore, this periodic expression of *NORM* may play a crucial role in regulating the cell cycle. Indeed, we found that when we depleted *NORM* cells, they were arrested at the G2/M phase and were unable to move to the G1 phase upon release. The arrest of cells may be due to the defective assembly of proteins required for mitotic progression. Bida *et al.* also demonstrated that a mitosis-associated long noncoding RNA (lncRNA), MA-linc1, is essential for mitosis. In the absence of lncRNA-MA, cells are unable to progress from mitosis to the G1 phase of the cell cycle.

We evaluated the role of *NORM* in regulating cellular proliferation and found that *NORM* plays a crucial part in this process, with depletion of *NORM* resulting in reduced cell proliferation. The G2 phase is a critical phase for cell proliferation, as it determines the cell's fate, whether it will progress into the M phase and divide into two daughter cells. Other evidence also suggests that lncRNA depletion causes cell cycle arrest, leading to a decrease in cellular

342 proliferation.(19). Reduced cellular proliferation was accompanied by an increase in the rate
343 of apoptosis and an increase in the level of DNA damage. When a cell is arrested at any
344 checkpoint for an extended period, the apoptotic cascade is activated. We also observed that
345 cells were arrested for a longer time in the G2/M phase. This arrest may have triggered the
346 apoptotic cascade, leading to an increased rate of apoptosis.

347 At the molecular level, a cell's entry into each phase is regulated by various types of cyclins,
348 cyclin-dependent kinases (CDKs), cyclin kinase inhibitors, and specific transcription factors.
349 We observe a significant change in the protein level of CDK1 upon *NORM* depletion. CDK1 is
350 a key regulator of the G2 and M phases of the cell cycle. It, along with cyclin A and Cyclin B,
351 regulates cell entry from the G2 phase to the M phase.(20–23). A decrease in the level of
352 CDK1 is one possible reason cells are arrested at the G2/M boundary, and this defect also
353 causes defects in mitotic cells.

354 Through RNA sequencing analysis and proteomics analysis, we found that pathways such as
355 the Regulation of mitotic cell cycle phase transition and the G2/M transition of the mitotic cell
356 cycle were affected. This suggests that *NORM* plays a crucial role in cell cycle progression.
357 DE mRNAs, such as BRCA1, FBXO6, and PCNT, which are involved in cell cycle regulation,
358 were significantly affected. BRCA1 plays a crucial role in regulating the cell cycle(24,25).
359 PCNT is a significant protein that helps in assembling the PCM complex for centrosome
360 maturation(26–28). Therefore, alterations in various genes related to cell cycle progression
361 could have resulted in changes to biological processes associated with the cell cycle.
362 Proteomics analysis also demonstrated that many proteins and the pathways related to cell
363 proliferation and cell cycle were affected.

364 In this study, we observed a significant decrease in Plk1 localization at the kinetochore. At
365 kinetochore Plk1 interacts with Bub1, BubR1 and MAD2 proteins(29–32). The interaction of
366 PLK1 with these proteins is essential for the nucleation of PCM components, including PCNT
367 (27,33). The interaction of Plk1 at the kinetochore facilitates the attachment of the kinetochore
368 to the microtubules (MT). Lera et al. observed a similar result, showing that Plk1 inhibition can
369 cause chromosome missegregation, characterized by lagging chromosomes (34). Therefore,
370 the reduced Plk1 localization at the kinetochore may have impacted the target proteins CENP-
371 U, BubR1, PICH, CLIP-170, CLASP2, Survivin, USP16, and RSF1, for example, including
372 Sgt1 phosphorylation, which could result in improper attachment of microtubules to the
373 kinetochore.(35). PLK1 phosphorylates CENP-Q by binding to CENP-U, and the absence of
374 phosphorylation can lead to chromosome mis-segregation(36).

375 The interaction between Bub1 and Plk1 is crucial for the proper segregation of chromosomes
376 during cell division. In our study, we observed that *NORM* depletion hampers the interaction

377 between these two proteins. It has been reported in studies that Bub1 becomes
378 phosphorylated at its T609 residue by CDK1, a crucial event for the binding of Bub1 to the
379 PBD domain of Plk1. So, the reduced interaction between Bub1 and Plk1 is a consequence
380 of the reduced CDK1-mediated phosphorylation on Bub1 T609. Plk1 also interacts with CENP-
381 U, along with Bub1, at the kinetochore for chromosome segregation; however, this study has
382 not explored the effect of the interaction between CENP-U and Plk1. In our study, we observed
383 that in the absence of *NORM*, the binding of Nsun2 on CDK1 mRNA was significantly reduced.
384 Other studies have also demonstrated the importance of Nsun2 binding to CDK1 mRNA and
385 its significance in the translation of CDK1 mRNA by mediating methylation. Although our data
386 suggested a direct interaction between the Nsun2 protein and *NORM*, we did not observe a
387 direct interaction between NORM and CDK1 mRNA, indicating that *NORM* lncRNA and CDK1
388 mRNA do not form an RNA-RNA interaction complex. This suggests possibilities other than a
389 direct RNA-RNA interaction. One of the limitations of our study is that we have not explored
390 in detail how exactly the *NORM* mediates the interaction between Nsun2 and CDK1 mRNA,
391 nor whether there is any change in the methylation of CDK1 mRNA. However, we speculate
392 that *NORM* acts as a Guide lncRNA for Nsun2 protein to mediate the methylation of CDK1
393 mRNA, thereby increasing its translation and subsequently phosphorylating Bub1 at T609.
394 Various studies have shown that lncRNAs can exert their functions by acting as a guide
395 molecule for the protein (37).

396

397 **MATERIALS AND METHODS:**

398 **Cell culture:**

399 HeLa cells and Wi-38 cells were cultured in DMEM and MEM, respectively, supplemented with
400 high glucose and 10% fetal bovine serum (FBS), as well as a penicillin-streptomycin antibiotics
401 solution (Gibco). Cells were maintained at 37°C in a humidified atmosphere of 5% CO2.

402 **Antisense oligonucleotide treatment**

403 Transient transfection of cells was performed using. For transfection, LNA GapmeRs
404 Phosphorothioate internucleosidic linkage-modified antisense oligonucleotides were diluted in
405 Opti-MEM. *NORM* Gapmers were used at a final concentration of 100 nM, twice (48 hours
406 apart) within a 24-hour gap, to deplete Human *NORM*.

407 **Flow cytometry:**

408 PI-Flow cytometry was used to analyze the distribution of cell cycle phases. Cells were
409 harvested using a scraper and then collected by centrifugation. Cells were washed with 1X

410 PBS (phosphate-buffered saline) and fixed in ethanol for at least 4 to 5 hours or overnight at
411 4 °C. Cells were washed two times with 1XPBS and then incubated in 500ul of 1X PBS
412 containing 0.1% Triton X-100, 20mg/ml propidium iodide, and 0.01mg/ml RNase A for 30 min
413 at 37ºC. It was followed by cell cycle analysis using a FACSCalibur (BD Bioscience), and the
414 data were analyzed using CellQuest Pro.

415 For BrdU-propidium iodide (PI), flow cytometry was performed as described earlier (Tripathi
416 et al., 2013). Briefly, S-phase cells were labeled with BrdU at a final concentration of 50 μM
417 and incubated for 1 hour at 37°C. Cells were further resuspended in chilled 0.9% NaCl and
418 then fixed in an equal volume of ethanol, followed by incubation at −20°C for 1 hour.
419 Furthermore, cells were resuspended and incubated in a 2N HCl + 0.5% Triton X-100 solution
420 for 30 minutes at room temperature, followed by washing in 0.1 M Sodium tetraborate solution.
421 Finally, the cells were resuspended in PBS/0.5% Tween-20 + 1% BSA and incubated with the
422 anti-BrdU antibody for 1 hour at RT. The cells were incubated in PBS + PI/Triton X-100 at
423 37°C for 15 min. Cells were analyzed using a FACScalibur flow cytometer (BD Bioscience),
424 and the data were analyzed with CellQuest Pro.

425 For mitotic cell counting, total cells were collected by trypsinization. It was followed by fixing
426 the cells in chilled 70% ethanol. Cells were permeabilized by using 0.25% Triton X-100. Cells
427 were incubated with H3ser10 antibody (Abcam, ab14955) for two hours at room temperature.
428 It was followed by brief washing and blocking of the cells with 1% BSA. Further, cells were
429 incubated with Alexa Fluor 488 secondary antibody for 30 minutes at room temperature.
430 Moreover, finally, cells were incubated with Propidium iodide (PI) containing RNase for 30
431 minutes. Cells were analyzed using a FACScalibur flow cytometer (BD Bioscience), and the
432 data were analyzed with CellQuest Pro.

433 To detect apoptosis, dual staining with Annexin V and propidium iodide (PI) was performed
434 according to the manufacturer's instructions (Invitrogen, cat. no R37174). Briefly, Wi-38 cells
435 were trypsinized, collected, and washed with ice-cold PBS. Cells were resuspended in 500 μL
436 of 1x binding buffer. A drop of Annexin-V FITC was added, and cells were incubated for 15
437 minutes at 25°C in the dark. 5 μL propidium iodide was added before acquiring the cells. Cells
438 were acquired using a BD FACScanto, and data were analyzed with CellQuest Pro.

439 **Total RNA extraction and quantitative real-time PCR (qRT-PCR):**

440 Total RNA was isolated from cells using Trizol reagent (Invitrogen) according to the
441 manufacturer’s instructions, and the concentration was estimated using a UV
442 spectrophotometer. Genomic DNA was digested by DNase I (Sigma) treatment. Total RNA
443 was subjected to first-strand cDNA synthesis using Multiscribe Reverse Transcriptase and

444 Random Hexamers (Invitrogen)**.** Transcript levels were quantified by qRT-PCR using gene-
445 specific primers.

446 **RNA-seq analysis:**

447 Whole-transcriptome analysis of control and *NORM*-depleted samples was performed on the
448 Illumina HiSeq 2500 platform to achieve high transcriptome coverage (50-100 million reads
449 per sample). Briefly, Total RNA was isolated by the RNeasy kit (Qiagen). RNA-seq libraries
450 were constructed using total RNA isolated from untreated and *NORM*-depleted samples with
451 the RNeasy kit (Qiagen). Samples were indexed with adaptors and submitted to paired-end
452 sequencing. RNA-seq reads were aligned with Tophat2.0.11 to the human genome. A
453 comparison of expression levels was calculated by using fragments per kilobase of transcripts
454 per million fragments mapped (FPKM). Gene ontology analysis was performed by using the
455 Database for Annotation, Visualization, and Integrated Discovery (DAVID) tool
456 (https://david.ncifcrf.gov).

457 **Quantitative proteomics by label-free quantitation mass spectrometry**

458 Human lung fibroblast primary cells (WI38) were seeded in 10 cm cell culture plates for both
459 the scrambled and NORM-depleted conditions. Cells were collected and pelleted in 1X PBS.
460 1X PBS was removed entirely, and the cell pellet was snap-frozen by liquid nitrogen for 20–
461 30 seconds and stored at -80 °C. Urea lysis buffer was used for cell lysis, and the cells were
462 sonicated to ensure complete lysis. Acetone precipitation was performed by incubating
463 overnight at -20 °C with acetone. Urea rehydration buffer was used for the elution of proteins,
464 followed by the removal of salts. An Amicon ultra-0.5 centrifugal filter unit with a 3 kDa cut-off
465 (UFC500394) was used for removing salt and concentrating the sample. Protein was
466 estimated using Pierce reagent, and bovine serum albumin (BSA) was used for plotting the
467 standard curve. An equal amount of protein (50 µg) was digested using the TFE-In solution
468 digestion protocol. Desalting and concentrating peptides or small proteins were performed
469 using a ZipTip with 0.6 µL C18 resin (ZTC18S096). Mass spectrometry sample preparation
470 was performed by adding 0.1% formic acid to dried protein samples. Samples were acquired
471 by injecting a 2 µL sample into the Thermo Scientific Orbitrap Fusion Tribrid LC-MS/MS
472 system. Raw files were transferred to the Proteome Discoverer software for analysis of the
473 sample.

474

475 **Cell proliferation assay:**

476 Cell viability was assessed using the 3-(4,5-dimethylthiazol-2-yl)-2,5-diphenyltetrazolium
477 bromide (MTT) assay. Briefly, after transfection with *NORM* ASO or scrambled oligos for 48

478 hours, HeLa cells were trypsinized, and a suspension of 5000 cells was seeded into a 96-well
479 plate. After 24 hours, 20 µL of MTT (5 mg/mL) was added and the cells were incubated for an
480 additional 4 hours. Then, 150 µL of isopropanol was added to dissolve the crystals. The
481 proliferation ability of cells was assessed at 0 hours, 24 hours, 48 hours, 72 hours, and 96
482 hours by incubating the cells at 37°C. Absorbance at 570 nm was determined
483 spectrophotometrically by using a microplate reader. Colony-forming ability was checked by
484 colony formation assay. Briefly, 1,000 cells were seeded in a six-well plate and maintained for
485 2 weeks, during which the media were replaced every 3 days. Colonies were fixed by PFA
486 and stained by using crystal violet in PBS for 30 minutes. The colony formation ability was
487 assessed by counting stained colonies.

488

489 **Immunoblotting**

490 Cells were washed twice with PBS and then collected by scraping. A lysis buffer containing
491 protease and phosphatase inhibitor was used for extraction. Loading dye was added directly
492 to the samples, and the samples were denatured by boiling for 5 min at 95°C. The total cell
493 lysate was subjected to SDS-polyacrylamide gel electrophoresis (SDS-PAGE), and proteins
494 were transferred to the PVDF membrane. The membrane was incubated with primary
495 antibodies overnight at 4°C. An appropriate secondary antibody was incubated for 1 hour at
496 room temperature. The antibodies used for immunoblotting were anti-CDK1(Cdc2) (1:1000;
497 Santa Cruz SC-54), anti-PARP (1:1000; Cell signaling technology, 9542), anti-Bax (1:500;
498 Santa Cruz sc493), anti-Bcl2 (1:500; Santa Cruz sc492), anti-Plk1 (1:1000 Abcam ab17056),
499 anti-Cyclin A (1:1000; Santa Cruz sc271682), anti-Cyclin B(1:1000; Santa Cruz sc7393), anti-
500 Cyclin E (1:1000; Santa Cruz sc377100), anti-CDK4(1:1000; Santa Cruz sc23896), anti-
501 Bub1(1:100 ab54893), H3ser10 antibody (1:1000; ab14955;), anti-α-Tubulin (1:5000; Sigma
502 T6199), Anti-mouse IgG, HRP-linked (1:5000; cell signalling technology; 7076), Anti-rabbit
503 IgG, HRP-linked (1:5000; cell signalling technology; 7074).

504 **Immunostaining:**

505 Immunofluorescence was performed as described earlier (Tripathi et al., 2013). Briefly, Wi-38
506 cells, grown on coverslips, were then fixed in 2% PFA for 20 minutes at room temperature
507 (RT) and permeabilized with 0.1% Triton X-100 for 10 minutes on ice. Cells were blocked by
508 incubating with 5% fetal bovine serum (FBS) at room temperature (RT) for 1 hour, followed by
509 incubation with the primary antibody for 2 hours at RT. Incubation with fluorescence-tagged
510 secondary antibody was performed for 1 hour at room temperature. Finally, cells were stained
511 with Hoechst and mounted in mounting media. The antibodies were used are Ki-67 (1:500;
512 Abcam; ab16667), anti-Plk1 (1:100 Abcam; ab17056), anti-α-Tubulin (1:1000; Sigma T6199),

513 anti-Bub1(1:100; Abcam; ab195268), anti-Pericentrin (1:200; Novus; NB 100-61071) CREST
514 (1:500; antibodiesinc; 115-234), Alexa flour 488 donkey anti-rabbit IgG (H+L) (1:1000;
515 Invitrogen; A21206), Alexa flour 594 donkey anti-mouse IgG (H+L) (1:1000; Invitrogen;
516 A21203) images were acquired on Zeiss microscope.

517 **RNA pulldown and Mass spectrometry analysis:**

518 *NORM* was cloned in a pGEMT vector. The plasmid was linearized by using the NcoI
519 restriction enzyme. Purified plasmids were then used for in vitro transcription with a Biotin RNA
520 labeling Mix (Roche). Biotin labeling was done by using T7 polymerase at 37°C for 6 hours.
521 In vitro transcribed RNA was then purified by passing it through a MicroSpin column (Illustra
522 MicroSpin G-25 columns, 27-5325-01, Merck). Fresh lysate was prepared by using Protein
523 extraction buffer (20 mM Tris HCl pH 7.5, 100 mM KCl,5 mM MgCl2,0.5% NP40) with
524 protease, phosphatase cocktail inhibitors, and RNase inhibitors. The lysate was precleared
525 using magnetic streptavidin Dynabeads (M-280 streptavidin, Cat. No. 11205D, Invitrogen).
526 Biotin-labeled RNA and lysate were incubated on a rotator for 2 hours. It was followed by the
527 addition of magnetic streptavidin Dynabeads to a mixture of RNA-lysate. It was further
528 incubated for 2 hours. Next, protein samples were separated by SDS-PAGE, and bands were
529 visualized by silver staining. For mass spectrometry analysis, the immunoprecipitated protein
530 was washed with 100 mM ammonium bicarbonate. Proteins were prepared for mass
531 spectrometry by digesting with RapiGest at 60°C for 30 minutes and then analysed by mass
532 spectrometry.

533 **RNA Immunoprecipitation:**

534 Cells were washed twice with ice-cold phosphate-buffered saline (PBS). Cells were irradiated
535 with 300mJ/cm^2 in a UV crosslinker. The cell lysate was prepared by using RSB100 lysis buffer
536 (100 mM Tris-Cl pH 7.4, 100 mM NaCl, 2.5 mM $MgCl_2$, 0.5% NP40, 0.5% Triton X-100) by
537 incubating on ice for 15 minutes. The lysate was centrifuged, and the supernatant was
538 collected. 0.1M DTT, RNase Inhibitor, and DNase I were added to the supernatant. The lysate
539 was precleared by incubating Protein G agarose beads (Pierce, Cat. No. 20398) at 4°C for 1
540 hour, rotating on a rotor shaker. Immunoprecipitation was performed by incubating an equal
541 amount of lysate with an anti-Plk1 antibody (1:100; Abcam, ab17056), anti-Nsun2 (1:100;
542 Abcam, ab259941), and a mouse IgG antibody (Negative control) overnight on a rotator
543 shaker at 4 °C. Next, protein G agarose beads were added and incubated further for 2 hours.
544 Co-immunoprecipitated RNA was isolated by resuspending the beads in 1 mL of Trizol
545 (Invitrogen). RNA was isolated according to the manufacturer's instructions. cDNA was
546 prepared using 5X PrimeScript RT Master Mix (Takara, cat. no RR036A-1).

547

548 **References:**

549 1. Pavletich NP. Mechanisms of cyclin-dependent kinase regulation: Structures of Cdks,
550 their cyclin activators, and Cip and INK4 inhibitors. J Mol Biol. 1999;287(5):821–8.

551 2. Giacinti C, Giordano A. RB and cell cycle progression. Oncogene. 2006;25:5220–7.

552 3. Holland AJ, Cleveland DW. Losing balance: the origin and impact of aneuploidy in
553 cancer. EMBO Rep [Internet]. 2012;13(6):501–14. Available from:
554 http://dx.doi.org/10.1038/embor.2012.55

555 4. Cleveland DW, Mao Y, Sullivan KF. Centromeres and kinetochores: From epigenetics
556 to mitotic checkpoint signaling. Cell. 2003;112(4):407–21.

557 5. Lara-gonzalez P, Pines J, Desai A. Spindle assembly checkpoint activation and
558 silencing at kinetochores. Semin Cell Dev Biol [Internet]. 2021;117:86–98. Available
559 from: https://doi.org/10.1016/j.semcdb.2021.06.009

560 6. Lara-gonzalez P, Westhorpe FG. The Spindle Assembly Checkpoint. Curr Biol
561 [Internet]. 2012;22(22):R966–80. Available from:
562 http://dx.doi.org/10.1016/j.cub.2012.10.006

563 7. Overlack K, Primorac I, Vleugel M, Krenn V, Maffini S, Hoffmann I, et al. A molecular
564 basis for the differential roles of Bubl and BubR1 in the spindle assembly checkpoint.
565 Elife. 2015;2015(4):1–24.

566 8. Yamagishi Y, Yang CH, Tanno Y, Watanabe Y. MPS1/Mph1 phosphorylates the
567 kinetochore protein KNL1/Spc7 to recruit SAC components. Nat Cell Biol.
568 2012;14(7):746–52.

569 9. Singh P, Pesenti ME, Maffini S, Srinivasamani A, Singh P, Pesenti ME, et al. BUB1
570 and CENP-U , Primed by CDK1 , Are the Main PLK1 Kinetochore Receptors in
571 Mitosis ll BUB1 and CENP-U , Primed by CDK1 , Are the Main PLK1 Kinetochore
572 Receptors in Mitosis. Mol Cell [Internet]. 2021;81(1):67-87.e9. Available from:
573 https://doi.org/10.1016/j.molcel.2020.10.040

574 10. Josue E, Nebreda AR, Fernandez M. A Two-Step Inactivation Mechanism of Myt1
575 Ensures CDK1 / Cyclin B Activation and Meiosis I Entry. Curr Biol. 2010;717–23.

576 11. Malumbres M. Cyclin-dependent kinases. Malumbres Genome Biol. 2014;1–10.

577 12. Xing J, Yi J, Cai X, Tang H, Liu Z, Zhang X, et al. NSun2 Promotes Cell Growth via
578 Elevating Cyclin-Dependent Kinase 1 Translation. Mol Cell Biol. 2015;35(23):4043–
579 52.

580 13. Tripathi V, Shen Z, Chakraborty A, Giri S, Freier SM, Wu X, et al. Long Noncoding
581 RNA MALAT1 Controls Cell Cycle Progression by Regulating the Expression of
582 Oncogenic Transcription Factor B-MYB. PLoS Genet. 2013;9(3).

583 14. Wang C, Yang Y, Zhang G, Li J, Wu X, Ma X, et al. Long noncoding RNA EMS
584 connects c-Myc to cell cycle control and tumorigenesis. PNAS. 2019;

585 15. Su C, Wang W, Mo J, Liu F, Zhang H, Liu Y, et al. Long noncoding RNA HOXC - AS3
586 interacts with CDK2 to promote proliferation in hepatocellular carcinoma. Biomark Res
587 [Internet]. 2022;1–15. Available from: https://doi.org/10.1186/s40364-022-00411-2

588 16. Singh P, Pesenti ME, Maffini S, Carmignani S, Hedtfeld M, Petrovic A, et al. BUB1
589 and CENP-U, Primed by CDK1, Are the Main PLK1 Kinetochore Receptors in Mitosis.
590 Mol Cell [Internet]. 2021;81(1):67-87.e9. Available from:
591 https://doi.org/10.1016/j.molcel.2020.10.040

592 17. Qi W, Tang Z, Yu H. Phosphorylation- and Polo-Box – dependent Binding of Plk1 to
593 Bub1 Is Required for the Kinetochore Localization of Plk1. Mol Biol Cell.
594 2006;17(August):3705–16.

595 18. Hao Q, Zong X, Sun Q, Lin Y, Song YJ, Hashemikhabir S, et al. The S-phase-induced
596 lncRNA SUNO1 promotes cell proliferation by controlling YAP1 / Hippo signaling
597 pathway. Elife. 2020;1–33.

598 19. Zhang X, Wu N, Wang J, Li Z. LncRNA MEG3 inhibits cell proliferation and induces
599 apoptosis in laryngeal cancer via miR-23a/APAF-1 axis. J Cell Mol Med.
600 2019;23(10):6708–19.

601 20. Ubersax JA, Woodbury EL, Quang PN. Targets of the cyclin-dependent kinase Cdk1.
602 Nature. 2003;859–64.

603 21. Porter LA, Donoghue DJ. Cyclin B1 and CDK1 : Nuclear localization and upstream
604 regulators Cyclin B1 and CDK1 : nuclear localization and upstream regulators. Prog
605 Cell Cycle Res. 2003;(February).

606 22. Gavet O, Pines J. Progressive Activation of CyclinB1-Cdk1 Coordinates Entry to
607 Mitosis. Dev Cell [Internet]. 2010;18(4):533–43. Available from:
608 http://dx.doi.org/10.1016/j.devcel.2010.02.013

609 23. Cerqueira A, Hunt S, Tardy C, Newton K, Santamarı D, Dubus P, et al. Cdk1 is
610 sufficient to drive the mammalian cell cycle. Nature. 2007;448(August):811–6.

611 24. Deng CX. BRCA1: Cell cycle checkpoint, genetic instability, DNA damage response

612 and cancer evolution. Nucleic Acids Res. 2006;34(5):1416–26.

613 25. Xu B, Kim S, Kastan MB. Involvement of Brca1 in S-Phase and G2-Phase
614 Checkpoints after Ionizing Irradiation. Mol Cell Biol. 2001;21(10):3445–50.

615 26. Kim J, Kim J, Rhee K. PCNT is critical for the association and conversion of centrioles
616 to centrosomes during mitosis. J Cell Sci. 2019;132(6).

617 27. Kim J, Lee K, Rhee K. PLK1 regulation of PCNT cleavage ensures fidelity of centriole
618 separation during mitotic exit. Nat Commun. 2015;

619 28. Tibelius A, Marhold J, Zentgraf H, Heilig CE, Neitzel H, Ducommun B, et al.
620 Microcephalin and pericentrin regulate mitotic entry via centrosome-associated Chk1.
621 J Cell Biol. 2009;185(7):1149–57.

622 29. Schmucker S, Sumara I. Molecular dynamics of PLK1 during mitosis. Mol Cell Oncol.
623 2014;(June):1–9.

624 30. Lee K, Rhee K. PLK1 phosphorylation of pericentrin initiates centrosome maturation
625 at the onset of mitosis. J Cell Biol. 2011;195(7):1093–101.

626 31. Gheghiani L, Loew D, Gavet O. PLK1 Activation in Late G2 Sets Up Commitment to
627 Mitosis. Cell Rep. 2017;2060–73.

628 32. Ikeda M, Tanaka K. Plk1 bound to Bub1 contributes to spindle assembly checkpoint
629 activity during mitosis. Sci Rep [Internet]. 2017;(September 2016):1–15. Available
630 from: http://dx.doi.org/10.1038/s41598-017-09114-3

631 33. Lee K, Rhee K. PLK1 phosphorylation of pericentrin initiates centrosome maturation
632 at the onset of mitosis. J Cell Sci. 2011;195(7):1093–101.

633 34. Lera RF, Norman RX, Dumont M, Dennee A, Martin-koob J, Fachinetti D, et al. Plk 1
634 protects kinetochore – centromere architecture against microtubule pulling forces.
635 EMBO Rep. 2019;1–16.

636 35. Liu XS, Song B, Tang J, Liu W, Kuang S, Liu X. Plk1 Phosphorylates Sgt1 at the
637 Kinetochores To Promote Timely. 2012;32(19):4053–67.

638 36. Kang YH, Park C, Kim T, Soung N, Bang JK, Kim BY, et al. Mammalian Polo-like
639 Kinase 1-dependent Regulation of the PBIP1-CENP-Q Complex at Kinetochores * □.
640 J Biol Chem [Internet]. 2011;286(22):19744–57. Available from:
641 http://dx.doi.org/10.1074/jbc.M111.224105

642 37. Zhao Z, Sentürk N, Song C, Grummt I. lncRNA PAPAS tethered to the rDNA

643 enhancer recruits hypophosphorylated CHD4 / NuRD to repress rRNA synthesis at
644 elevated temperatures. GENES Dev. 2018;836–48.

645

FIG 1: *NORM* is up-regulated during the G2 phase of the cell cycle and promotes G2/M transition

(A)*NORM* location and Histone acetylation and methylation were shown using the UCSC browser.

(B) Coding potential calculation of *NORM*, JUND and MALAT1 were used as coding and non-coding control transcripts.

(C) Subcellular localization of *NORM*. MALAT1 and RNR were used as nuclear and cytoplasmic markers, respectively.

(D) Cell phase-specific expression of *NORM* in HeLa cells.

(E) Knockdown efficiency of *NORM* in Wi-38 cells calculated by using qRT-PCR.

(F) PI-flow cytometry analysis of SCR vs. *NORM* depleted cells in WI-38 and HeLa cells.

(G) Cell cycle analysis of cells by BrdU-PI flow cytometry analysis of SCR vs *NORM* depleted condition in WI-38 cells.

(H) The percentage of the cell population of different phases in SCR vs. *NORM* knockdown samples.

(I) PI flow cytometry analysis of Nocodazole block and followed by a release in SCR vs *NORM* depleted HeLa cells.

(J) Quantitation of the percentage cell population of Nocodazole block, followed by a release in SCR vs *NORM* depleted HeLa cells.

(K) Immunoblot of different Cyclins and CDKs in SCR and *NORM* depleted WI-38 cells.

(L)Flow cytometry analysis of control and *NORM* depleted cells. H3ser10 was used as a mitotic marker.

(M) The percentage of cell population in the mitotic phase of control and *NORM*-depleted cells.

(N) Immunoblot analysis of Phospho-Histone H3 (p-H3 ser10) in control vs *NORM* depleted Wi-38 cells.

MS Excel was used to plot the mean (+SEM) of relative expression (n=3) and to calculate p-value (ns = $p>0.05$, * = $p \leq 0.05$, ** = $p \leq 0.01$, *** = $p \leq 0.001$ and **** = $p \leq 0.0001$).

FIG2: Loss of *NORM* affects cellular proliferation with an increase in apoptosis

(A) Ki-67 Immunostaining of SCR and *NORM* depleted cell in Wi-38.

(B) Quantitation of the percentage of Ki-67 population in SCR and NORM depleted Wi-38 cells.

(C) Depletion of *NORM* decreases cell survival as shown by the MTT assay.

(D) Colony formation assay to check colony formation ability of cells in SCR and *NORM* depleted cells.

(E) Quantitation of the Number of colonies observed in SCR and *NORM* depleted cells.

(F) Annexin V-PI flow cytometry analysis of live, early apoptotic and dead cell population in SCR and *NORM* depleted Wi-38 cells.

(G) Quantitation of the percentage of Early apoptotic and late apoptotic population in SCR and *NORM* knockdown cells.

(H) Immunoblot analysis of apoptotic markers in SCR and *NORM* depleted cells in Wi-38 cells.

MS excel was used to plot the mean (+SEM) of relative expression (n=3) and to calculate p value (ns = $p>0.05$, * = $p \leq 0.05$, ** = $p \leq 0.01$, *** = $p \leq 0.001$ and **** = $p \leq 0.0001$).

FIG 3: Loss of *NORM* leads to gene expression changes at the global transcriptomic and proteomic level

(A) Clustered Heatmap showing differential expression of genes in SCR and *NORM* depleted cells.

(B) Gene ontology analysis of the biological pathway of downregulated genes in RNA-seq in SCR and *NORM* depleted cells.

(C)Gene ontology analysis of the biological pathway of upregulated genes in RNA-seq in SCR and *NORM* depleted cells.

(D) Clustered Heatmap of proteins in SCR and *NORM* depleted cells.

(E) Upregulated and Downregulated proteins in proteomics analysis in SCR and *NORM* depleted cells.

(F) Gene ontology analysis of proteomics data of SCR and *NORM* depleted cells showing the biological process affected upon *NORM* depletion

FIG4: *NORM* interacts with cell cycle regulatory proteins for chromosome segregation and cell cycle regulation

(A)SDS-PAGE Gel image of *NORM* pulldown samples followed by a silver staining.

(B) List of interacting protein partners of *NORM* identified by mass spectrometry.

(C) Western blotting analysis of RNA pull-down samples followed with Plk1 and Nsun2 specific antibodies.

(D) RNA immunoprecipitation analysis of *NORM* and Plk1.

(E) Immunoblotting of PLK1 in SCR and *NORM* depleted cells.

(F) Immunofluorescence analysis of Plk1 and CREST at different phases of mitosis in SCR and *NORM* depleted cells.

(G) Representative image of Plk1 and CREST immunofluorescence staining at prometaphase in SCR and *NORM* depleted cells.

(H)Quantitation of intensity of Plk1 at the kinetochore normalized with CREST in SCR and *NORM* depleted cells.

(I) Immunofluorescence staining of alpha tubulin and PCNT to assess the chromosome mis-segregation in SCR and *NORM* depleted cells.

(J) Quantitation of the percentage of cells showing chromosome mis-segregation.

Graph Prism Pad was used to plot mean (+ SEM) of relative expression (n=97) and to calculate p-value. The Mann-Whitney U test was used. p-value < 0.05 were statistically significant. *p≤ 0.05, **p≤0.01, ***p≤0.001, ****p≤ 0.0001.

FIG 5: *NORM* depletion hampered the interaction between PLK1 and Bub1

(A) String analysis of Plk1 interacting proteins.

(B) Immunofluorescence staining of Bub1 and CREST in SCR and *NORM* depleted cells.

(C) Quantitation of intensity of Bub1 at kinetochore normalized with CREST in SCR and *NORM* depleted cells. Graph Prism Pad was used to plot the mean (+ SEM) of relative expression (n = 100) and to calculate the p-value. The Mann-Whitney U test was used. p-value < 0.05 were statistically significant. *p≤ 0.05, **p≤0.01, ***p≤0.001, ****p≤ 0.0001.

(D) Immunoblotting of Bub1 in SCR and *NORM* depleted cells.

(E)Co-immunoprecipitation assay of PLK1 with Bub1 in control and *NORM* depleted cells.

(F) Reverse Co-Immunoprecipitation assay of Bub1 and PLK1 in SCR and *NORM* depleted cells.

(G, H) Co-Immunoprecipitation assay to check the phosphorylation of Bub1(T609) by using the antibody anti-MPM2 in control and *NORM* depleted conditions.

FIG 6: *NORM* mediate the binding of Nsun2 on CDK1 mRNA to stabilize CDK1 protein

(A) RNA pulldown of *NORM* followed by immunoblotting of Nsun2 specific antibody.

(B) immunoblotting of Nsun2 in SCR and *NORM* depleted cells.

(C) Immunoprecipitation assay of Nsun2.

(D) RNA immunoprecipitation of Nsun2 to check the enrichment of CDK1 mRNA in SCR and *NORM* depleted cells.

(E) Immunoblotting assay of CDK1 in control and *NORM* depleted samples.

MS excel was used to plot the mean (+SEM) of relative expression (n=3) and to calculate p value (ns = $p>0.05$, * = $p \leq 0.05$, ** = $p \leq 0.01$, *** = $p \leq 0.001$ and **** = $p \leq 0.0001$

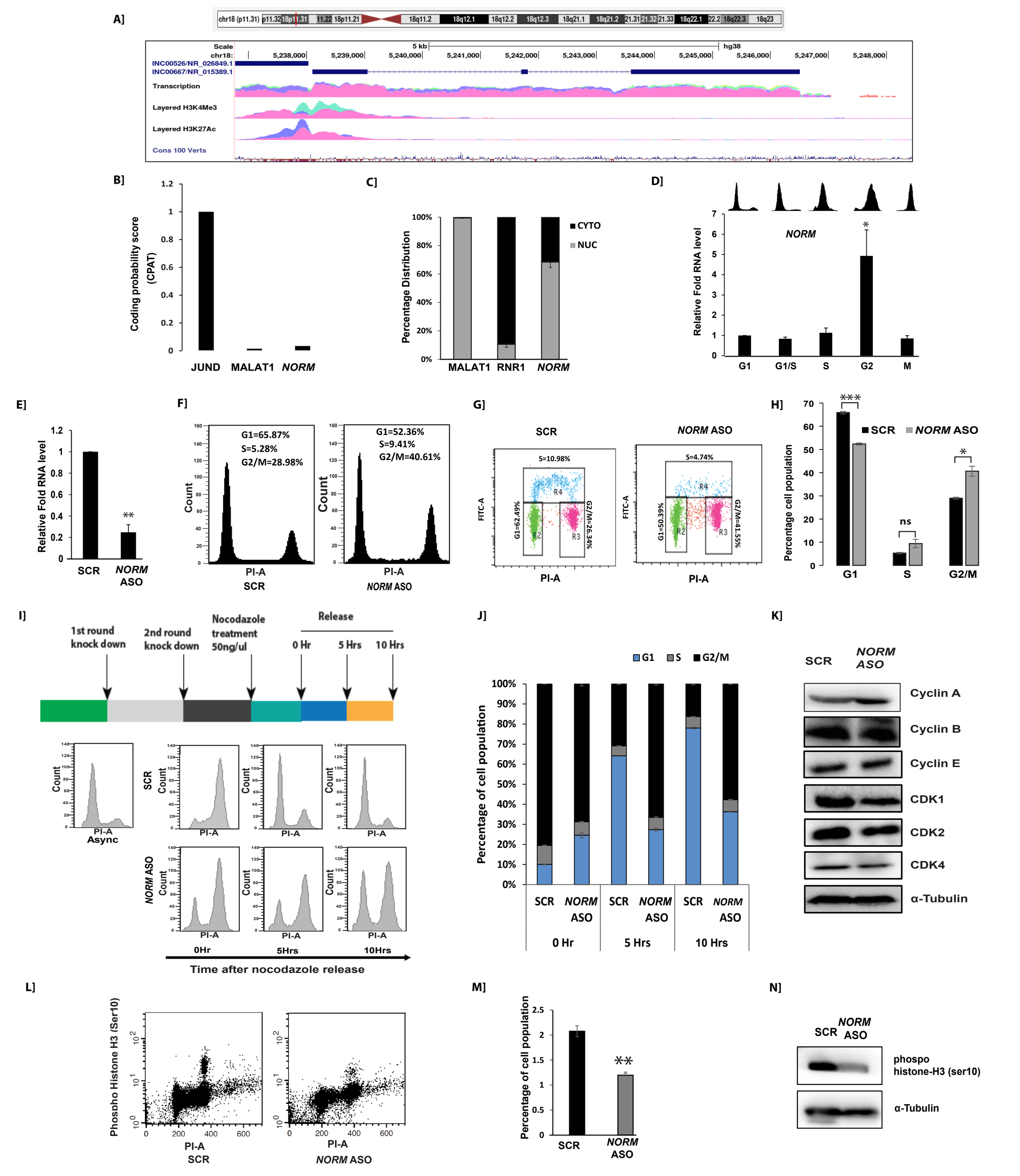
A]
chr18 (p11.31)
Scale
chr18:
5 kb
hg38
INC00526/NR_026849.1
INC00667/NR_015389.1
Transcription
Layered H3K4Me3
Layered H3K27Ac
Cons 100 Verts
B]
Coding probability score (CPAT)
JUND
MALAT1
NORM
C]
Percentage Distribution
CYTO
NUC
MALAT1
RNR1
NORM
D]
Relative Fold RNA level
NORM
G1
G1/S
S
G2
M
E]
Relative Fold RNA level
SCR
NORM ASO
F]
G1=65.87%
S=5.28%
G2/M=28.98%
G1=52.36%
S=9.41%
G2/M=40.61%
Count
PI-A
SCR
NORM ASO
G]
SCR
NORM ASO
S=10.98%
S=4.74%
FITC-A
PI-A
H]
Percentage cell population
SCR
NORM ASO
ns
G1
S
G2/M
I]
1st round knock down
2nd round knock down
Nocodazole treatment 50ng/ul
Release
0 Hr
5 Hrs
10 Hrs
Count
PI-A
Async
SCR
NORM ASO
0Hr
5Hrs
10Hrs
Time after nocodazole release
J]
G1
S
G2/M
Percentage of cell population
SCR
NORM ASO
0 Hr
5 Hrs
10 Hrs
K]
SCR
NORM ASO
Cyclin A
Cyclin B
Cyclin E
CDK1
CDK2
CDK4
α-Tubulin
L]
Phospho Histone H3 (Ser10)
PI-A
SCR
NORM ASO
M]
Percentage of cell population
SCR
NORM ASO
N]
SCR
NORM ASO
phospho histone-H3 (ser10)
α-Tubulin

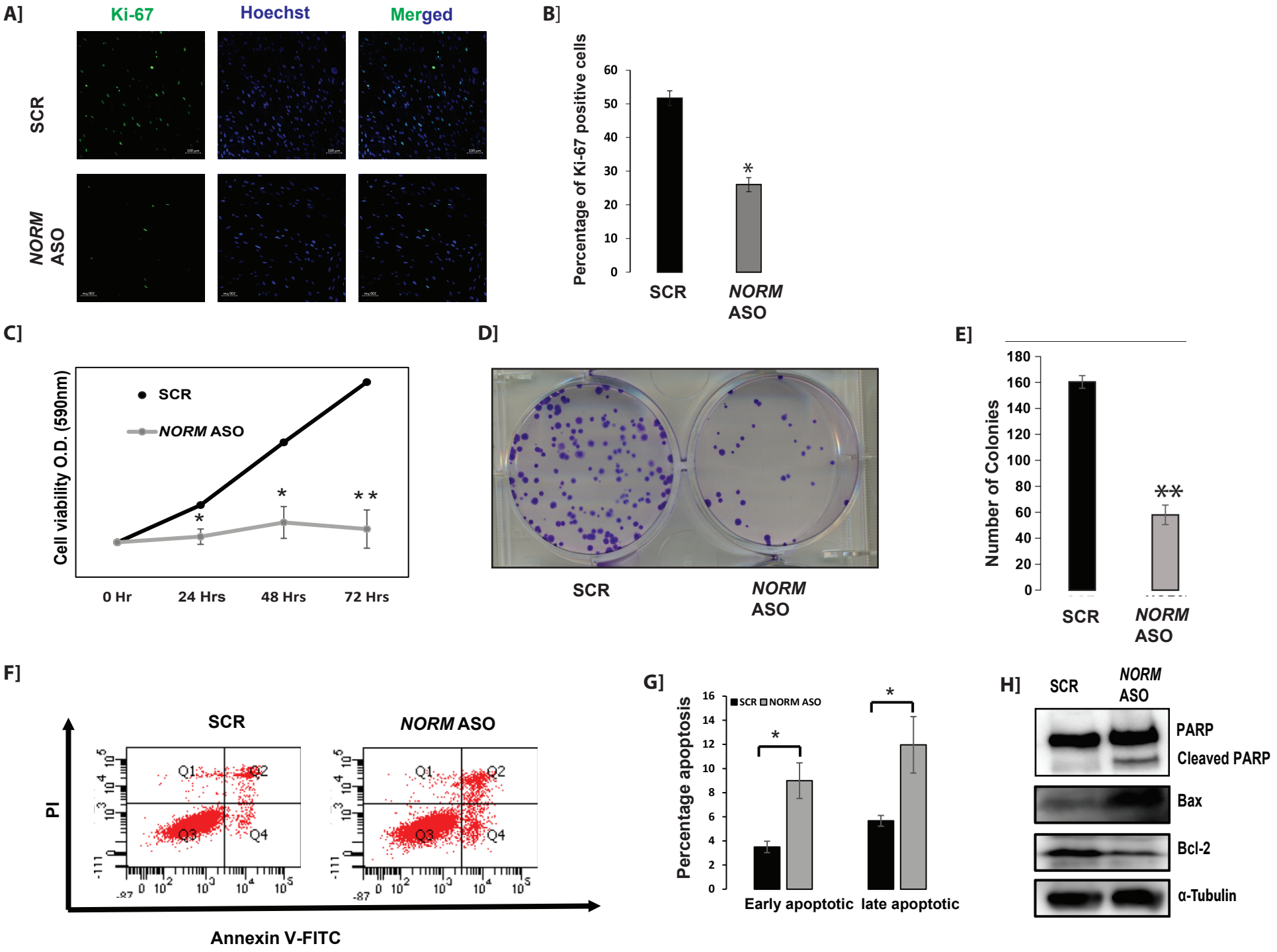
A]
Ki-67
Hoechst
Merged
SCR
NORM ASO
B]
Percentage of Ki-67 positive cells
60
50
40
30
20
10
0
*
SCR
NORM ASO
C]
Cell viability O.D. (590nm)
SCR
NORM ASO
*
*
* *
0 Hr
24 Hrs
48 Hrs
72 Hrs
D]
SCR
NORM ASO
E]
Number of Colonies
180
160
140
120
100
80
60
40
20
0
**
SCR
NORM ASO
F]
SCR
NORM ASO
PI
Q1
Q2
Q3
Q4
Annexin V-FITC
G]
Percentage apoptosis
SCR
NORM ASO
*
*
Early apoptotic
late apoptotic
H]
SCR
NORM ASO
PARP
Cleaved PARP
Bax
Bcl-2
α-Tubulin

A]

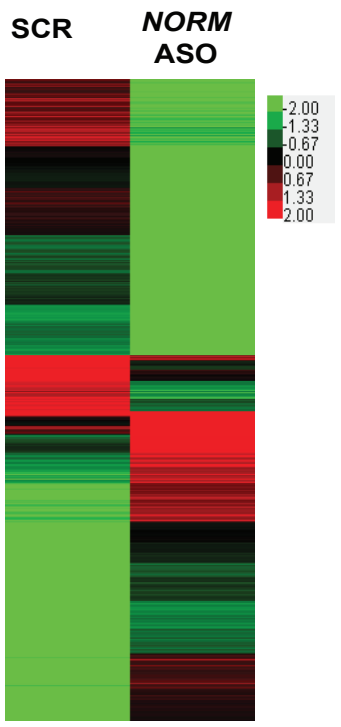

B]

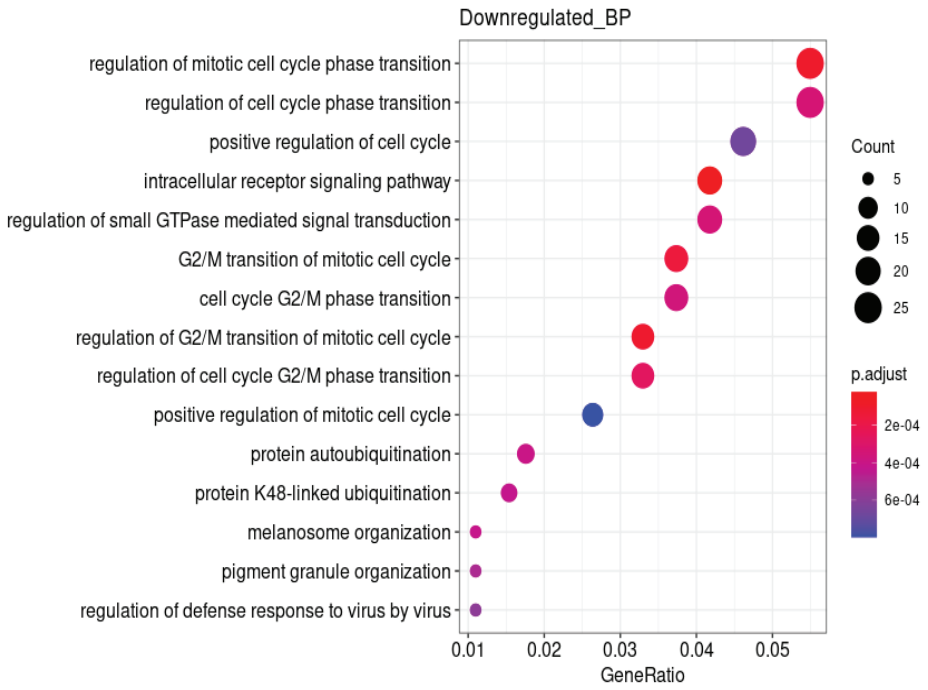

C]

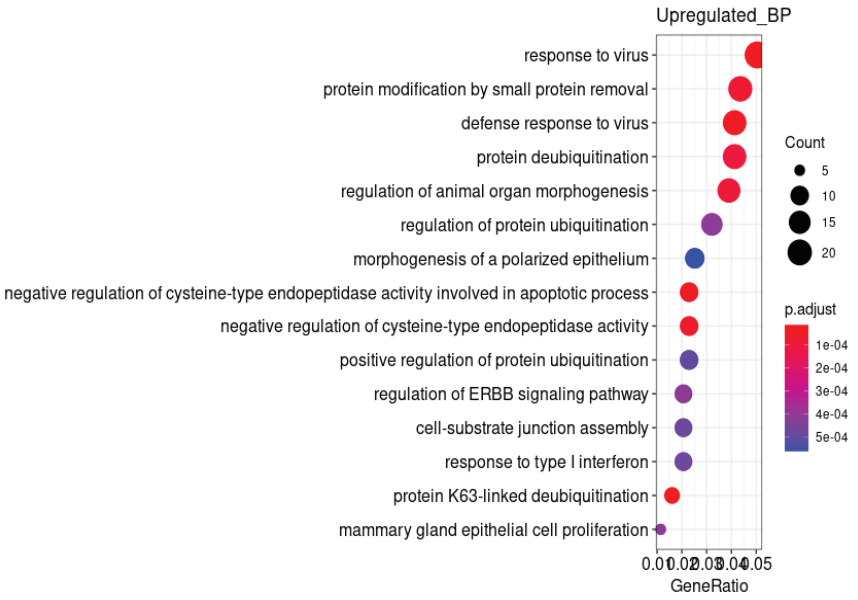

D]

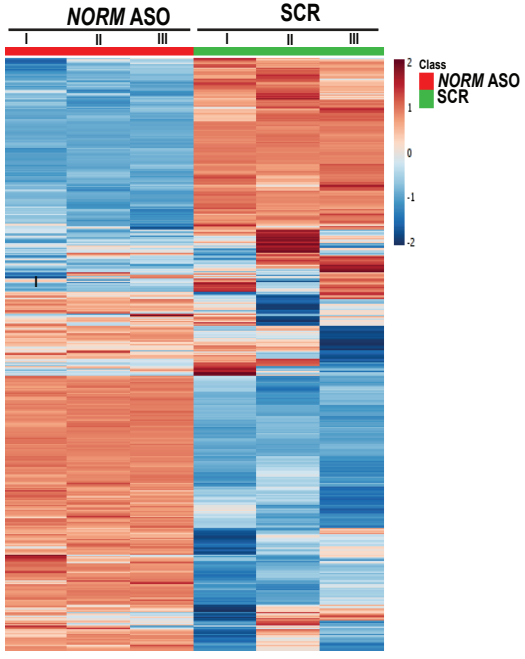

E]

Upregulated

Gene	Fold change
TGM2	18.648
PSMD1	18.52
CLTC	15.713
PSMD2	14.44
PSMA4	12.72
ANXA4	12.352
BUB3	11.486
BANF1	11.348
RCC1	10.743
DDB1	9.771
PRKDC	9.565
DYNC1H1	9.426
CTTN	9.028
NUP50	6.697
SBDS	6.387
PSMB1	6.372
GNAI2	6.25
HMGA2	6.021

Downregulated

Protein	Fold change
PDGFRB	0.016
PTMS	0.025
COL1A1	0.096
CD2AP	0.131
LAMB2	0.133
YWHAB	0.191
COL1A2	0.242
CDK1	0.263
RAD21	0.285
PPP2R5D	0.296
MCM3	0.382
RBX1	0.397
YWHAG	0.422
SMC4	0.435
CCDC124	0.436
YWHAE	0.438
MCM5	0.48

F]

Downregulated

Pathway	Count
negative regulation of apoptotic process	26
cell proliferation	22
negative regulation of ubiquitin-protein ligase activity involved in mitotic cell cycle	17
positive regulation of ubiquitin-protein ligase activity involved in regulation of mitotic cell cycle transition	17
anaphase-promoting complex-dependent catabolic process	17
DNA damage response, detection of DNA damage	7
mitotic nuclear envelope disassembly	6
mitotic spindle organization	5
mitotic spindle assembly	5

Upregulated

Pathway	Count
PI3K-Akt signaling pathway	9
cell division	8
Cell cycle	8
cell migration	5
G2/M transition of mitotic cell cycle	4
regulation of actin cytoskeleton organization	3
positive regulation of protein insertion into mitochondrial membrane involved in apoptotic signaling pathway	3
positive regulation of DNA biosynthetic process	2

A]

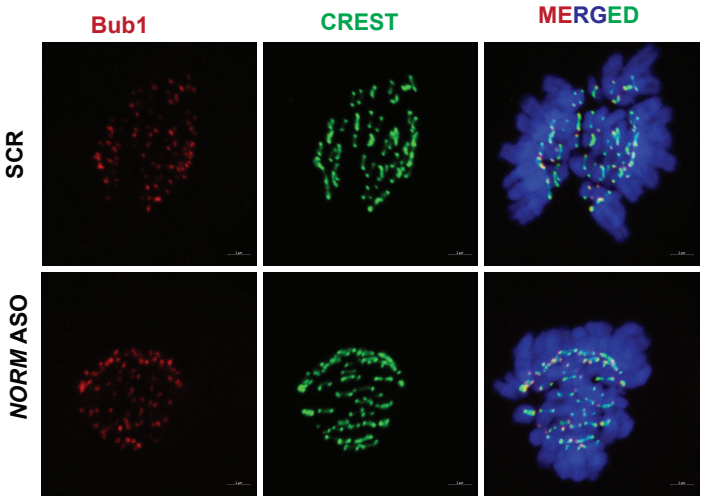
Bub1
CREST
MERGED
SCR
NORM ASO

C]

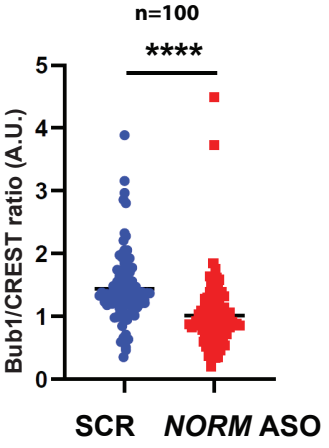
n=100
****
Bub1/CREST ratio (A.U.)
0
1
2
3
4
5
SCR
NORM ASO

D]

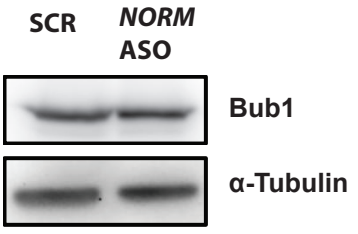
SCR
NORM ASO
Bub1
α-Tubulin

B]

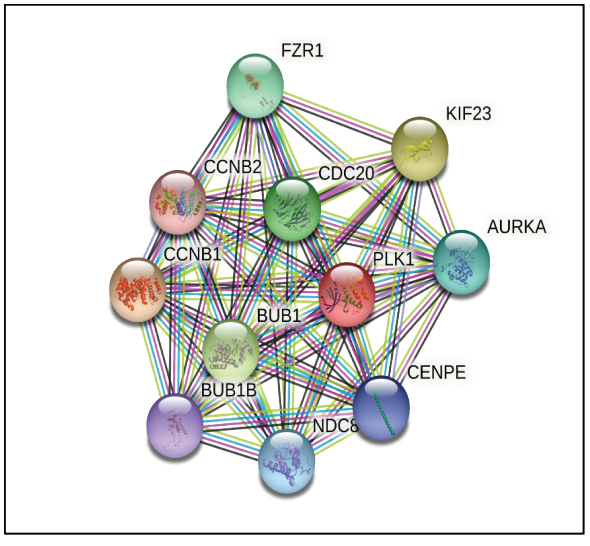
FZR1
KIF23
CCNB2
CDC20
AURKA
CCNB1
PLK1
BUB1
CENPE
BUB1B
NDC8

E]

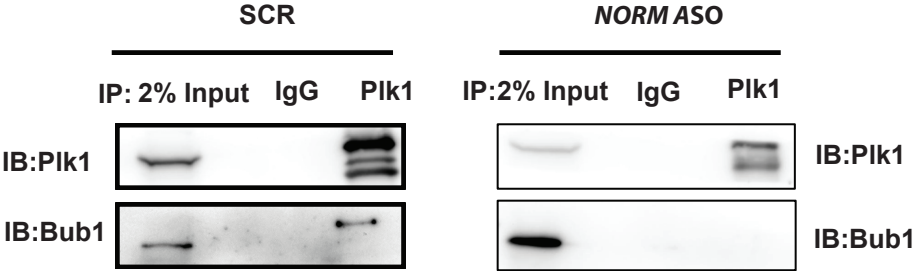
SCR
NORM ASO
IP: 2% Input
IgG
Plk1
IP:2% Input
IgG
Plk1
IB:Plk1
IB:Bub1
IB:Plk1
IB:Bub1

F]

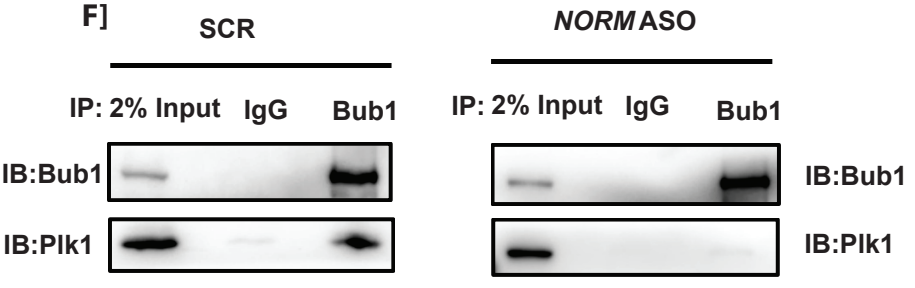
SCR
NORM ASO
IP: 2% Input
IgG
Bub1
IP: 2% Input
IgG
Bub1
IB:Bub1
IB:Plk1
IB:Bub1
IB:Plk1

G]

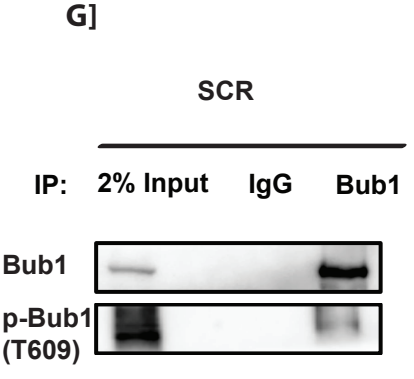
SCR
IP:
2% Input
IgG
Bub1
Bub1
p-Bub1
(T609)

H]

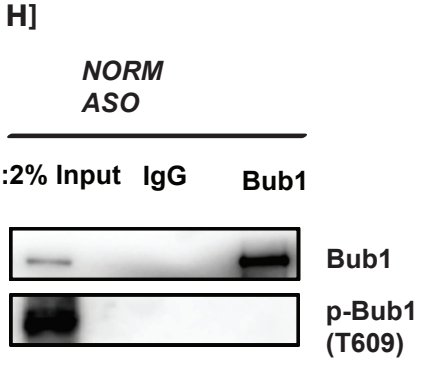
NORM
ASO
IP:2% Input
IgG
Bub1
Bub1
p-Bub1
(T609)

A]

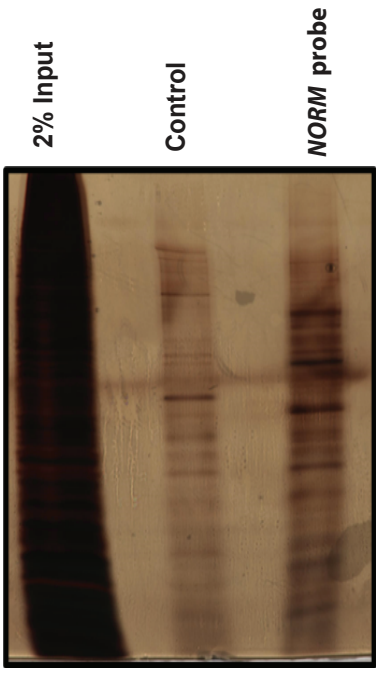

B]

Gene	Sum PEP score
XRN2	5.424
FUS	3.806
GNL3	9.488
KHDRBS1	5.627
NSUN2	3.706
ARHGEF2	1.483
SPOUT1	1.524
XRCC6	5.008
CALM2	7.023
CDC5L	3.339
GAPDH	2.324
MRPS26	3.483
PLK1	1.833
RPS27A	2.352
RPS6	8.711
TUBA1B	18.025
TUBB	20.338

C]

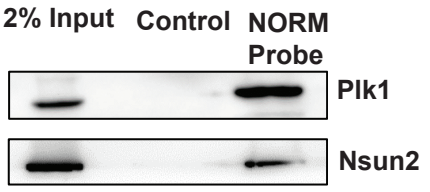

D]

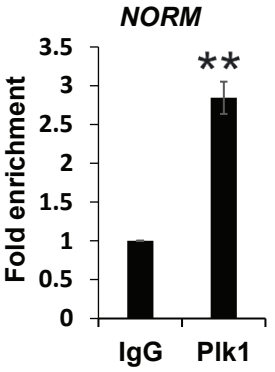

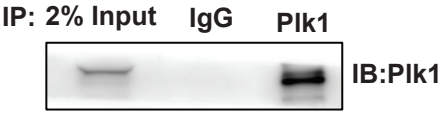

E]

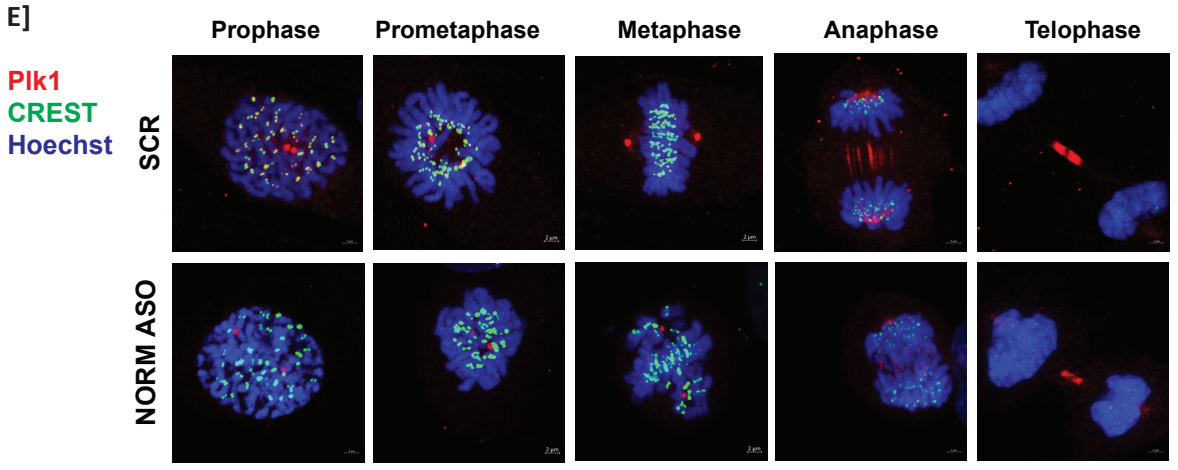

F]

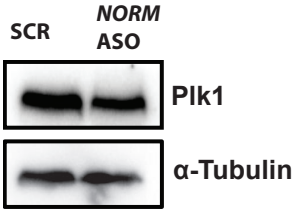

G]

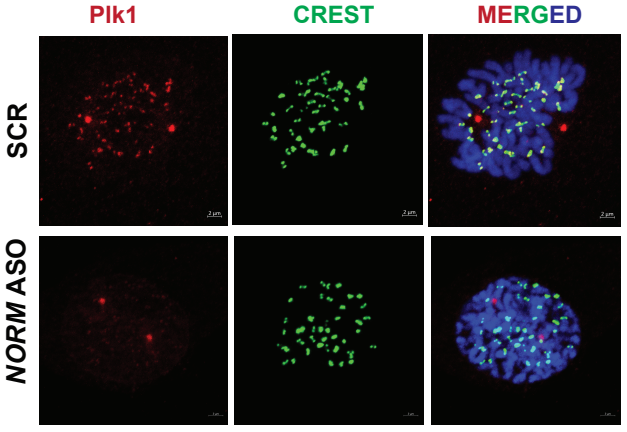

H]

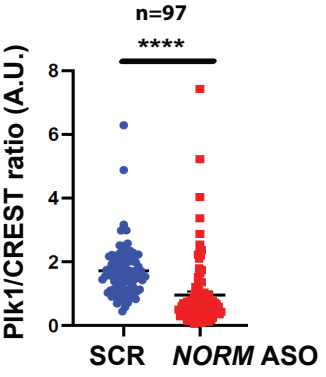

I]

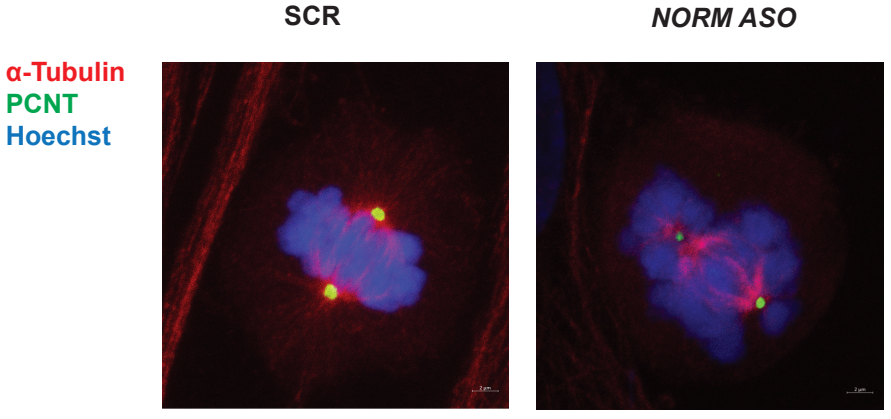

J]

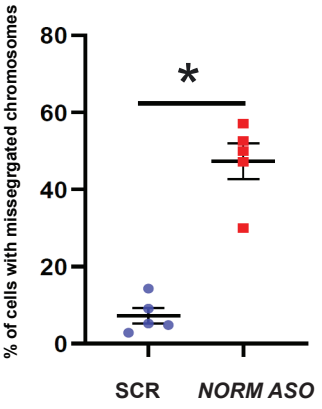

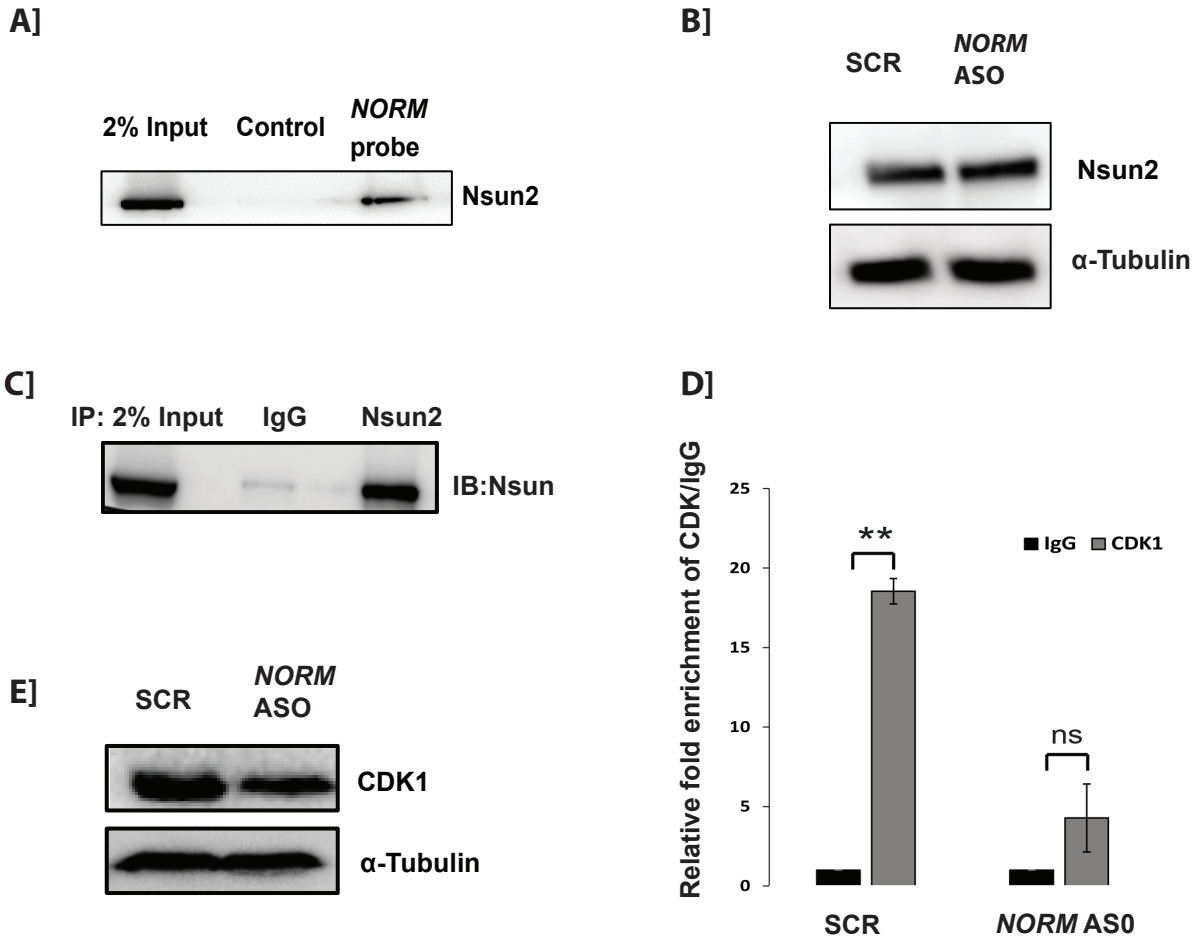
A]
2% Input
Control
NORM probe
Nsun2
B]
SCR
NORM ASO
Nsun2
α-Tubulin
C]
IP: 2% Input
IgG
Nsun2
IB:Nsun
D]
Relative fold enrichment of CDK/IgG
25
20
15
10
5
0
**
ns
IgG
CDK1
SCR
NORM AS0
E]
SCR
NORM ASO
CDK1
α-Tubulin